

## NONLINEAR BENDING ANALYSIS OF A LAMINATED COMPOSITE PLATE USING A REFINED ZIG-ZAG THEORY

M. J. Khoshgoftar,<sup>1\*</sup> M. Karimi,<sup>1</sup> and S. Seifoori<sup>2</sup>

**Keywords:** zig-zag theory, laminated composites, nonlinear analysis, shear-deformation theory.

*A modified zig-zag theory was used to investigate the bending behavior of composite plates and sandwich structures. The theory is based on the first-order shear-deformation theory on some piecewise linear functions for in-plane displacements. This theory does not depend on the shear correction factor and can be applied to various engineering problems associated with the structural dynamics. The nonlinear strain terms in the von Kármán compatibility equation were taken into account to calculate accurate results at large deformation. The governing equations and associated boundary conditions were derived using the principle of virtual work. The calculated numerical results are compared with those of other theories, and an excellent agreement between them was found. The figures and tables presented illustrate the superiority of the model considered in predicting the stress and displacement fields. The model proposed is applicable to nonlinear problems with large deflections.*

### 1. Introduction

Recently, the use of multilayered composites and sandwich materials various industries has significantly increased. Some advantages of the materials is a high corrosion resistance and high stiffness-to-weight and strength-to-weight ratios.

Various theories have been adopted for modeling their mechanical behavior. Models based on the Kirchhoff hypothesis, the shear-deformation theory, layerwise theories, the finite-element modeling, nonlinear theories, and mixed theories are some examples of them. Auricchio et al. [1] have presented a mixed variational theory based on the dimension reduction method for a multilayer anisotropic plate. They showed the power of their formulation by applying it to the displacement field. Fares and Elmarghany [2] published a modified mixed variational formulation of a refined nonlinear zig-zag theory for a laminated composite plate.

---

<sup>1</sup>Department of Mechanical Engineering, Faculty of Engineering, Arak University, Arak 38156- 88349, Iran

<sup>2</sup>Department of Mechanical Engineering, Faculty of Engineering, Vali-e-Asr University of Rafsanjan, Iran

\*Corresponding author; e-mail: mj.khoshgoftar@gmail.com, m-khoshgoftar@araku.ac.ir

There are different numerical methods for analyzing structures, e.g. the FEM, the mesh-free method, and isogeometric methods. The latter ones are designed by combining computer-aided and finite-element analyses, and it significantly reduces the error in the representation of the computational domain [3]. Pavan et al. [4] proposed an isogeometric collocation for a linear static bending analysis of laminated composite plates. A finite-element nonlinear zig-zag theory for laminated anisotropic shell was formulated by Chaudhuri [5]. He assumed its transverse inextensibility, vanishing normal transverse strains, and a layerwise constant shear-angle theory, also known as the zig-zag theory. The perturbation method was also used to solve governing equations. A thick cylinder of finite length was analyzed by Khoshgoftar et al. [6, 7] with the perturbation method.

A geometrically nonlinear analysis of beams, plates, and shells within the framework of the first order shear deformation theory (FSDT) was presented by Kreja [8]. He focused on the large-rotation finite-element analysis of laminated composite plates and shells. A nonlinear analysis of composite and sandwich plates based on a high-order theory considering the realistic variation of in-plane and transverse displacements across their thickness was published by Ganapathi et al. [9]. They presented a nonlinear dynamic analysis and introduced a geometrical nonlinearity for a laminate. A nonlinear electromechanically coupled zig-zag theory was developed by Kapuria and Achary for hybrid piezoelectric plates [10, 11]. They considered the von Kármán geometrical nonlinearity and obtained the initial buckling response of symmetrically laminated plates.

The classical shell theories neglect the rotary inertia and shear deformation effects and overestimate the natural frequencies of laminated anisotropic and moderately thick plates and shells. Three parameters are utilized in them to consider the deformation of shells. According to the geometrically nonlinear terms in these theories, they can be divided into two groups; those that maintain only the von Kármán-type nonlinear terms (involving only the normal displacement) and those that also keep nonlinear terms for two in-plane displacements. The theories that consider only the von Kármán-type nonlinear terms are accurate only at small displacement. Several nonlinear higher-order shear deformation theories have been developed for different laminated shells and plates with account their thickness deformations [12-14].

A nonlinear bending analysis of a simply supported symmetrically laminated plate based on a higher-order displacement theory was presented by Savithri and Varadan [15]. They used the single-mode Galerkin approach and the Newton–Raphson method for solving nonlinear governing equations.

The first-order zig-zag theory of laminates and the associated finite-element model for an analysis of moderately thick laminated beams was presented by Averill [16]. The accuracy of the new discrete-layer finite-element model was investigated in static and vibration analyses of thin and moderately thick laminated beams with delaminations and ply damage. This work was extended to a higher-order zig-zag laminate theory and its derivatives [17]. Di Sciuva [18] considered a multilayered anisotropic composite plate with a piecewise cubic displacement field and von Kármán nonlinear strain–displacement relations. Di Sciuva et al. [19] presented a nonlinear third-order theory of multilayered anisotropic shallow shells with damaged interfaces. Their theory allows for jumps in in-plane displacements when interlayer slips are present. Tessler et al. [20] introduced a refined zig-zag theory based on the Timoshenko beam theory for composite and sandwich beams and developed their theory for laminated composite and sandwich plates [21]. Ascione and Gherlone [22] published a nonlinear refined zig-zag theory based on the von Kármán strain field and the first-order shear deformation theory. It is more accurate than the Timoshenko beam theory for beams with a low slenderness ratio and thick face sheets, especially in the case of a high face-to-core stiffness ratio.

There can also be found size-dependent theories in the literature [23, 24]. Nonlocal theories [25], modified strain gradient theories [26, 27], and elasticity solutions [28] for sandwich panels are published frequently for different goals. The material type is another topic in the literature. Sandwich panels with a soft core [29, 30] and piezoelectric layers [31, 32], and nanoplatelets like graphene ones [33] are some examples with different materials.

In this paper, the nonlinear modified zig-zag theory is employed for a static analysis of multilayered composites. The applied theory is formulated based on the first-order shear-deformation theory and some piecewise linear functions for in-plane displacements. In contrast to the first-order shear-deformation theory, this theory does not depend on the shear correction factor and is applicable to various engineering problems associated with the structural dynamics. The nonlinear strain terms in the von Kármán compatibility equation are taken into account to obtain accurate results at large strains. One major benefit arising from the analytical form of this new theory is its ideal suitability for the finite-element modeling, where the kinematic approximations need not to exceed the C0 continuity. More accurate results of a less solution time are the main advantage of the current theory.

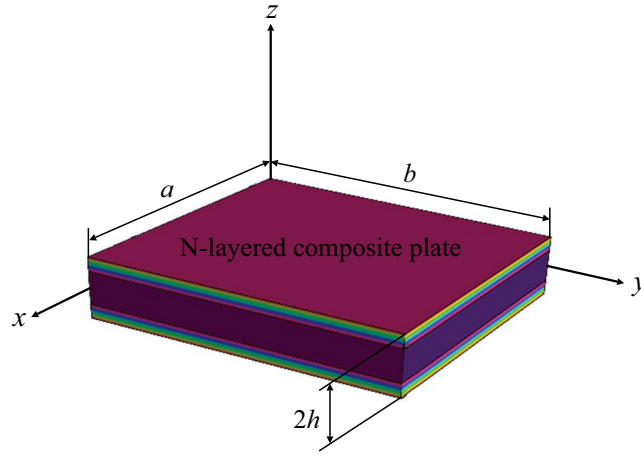


Fig. 1. Problem domain.

## 2. Formulation

Let us consider a composite plate with  $N$  layers. The domain  $\Omega$  of the plate considered is plotted in Fig. 1, and its analytical expression is.

$$\Omega = \{(x, y, z); -h \leq z \leq h\}. \quad (1)$$

The displacement field of the plate can be expressed using the modified zig-zag theory [21] according to different parameters of its midsurface in the following form:

$$\begin{aligned} u^{(k)}(x, y, z) &\equiv u_0(x, y) + z\theta_x(x, y) + \phi_x^{(k)}(z)\psi_x(x, y), \\ v^{(k)}(x, y, z) &\equiv v_0(x, y) + z\theta_y(x, y) + \phi_y^{(k)}(z)\psi_y(x, y), \\ w^{(k)}(x, y, z) &\equiv w_0(x, y), \end{aligned} \quad (2)$$

where  $u^{(k)}$ ,  $v^{(k)}$ , and  $w^{(k)}$  are the displacements of an arbitrary point in the  $x$ ,  $y$ , and  $z$ -axis;  $u_0(x, y)$  and  $v_0(x, y)$  are the uniform in-plane displacements in the  $x$  and  $y$  direction, respectively;  $w_0(x, y)$  is the out-of-plane displacement of the midplane in the  $z$ -direction;  $\theta_x(x, y)$  and  $\theta_y(x, y)$  are the rotation angles of plate cross-section in the  $xz$  and  $yz$  planes, respectively;  $\phi_x^k(z)$  and  $\phi_y^k(z)$  are the zig-zag functions in a  $k$ th layer, which are piecewise linear across the thickness of the composite plate. The functions  $\psi_x(x, y)$  and  $\psi_y(x, y)$  are the spatial amplitudes of zig-zag displacements, and, together with the other five kinematic variables, they are unknowns in the analysis. The first-order shear-deformation theory (FSDT) arises when the zig-zag functions vanish. These functions can be defined as [21]

$$\begin{aligned} \phi_x^{(k)} &\equiv \frac{1}{2}(1 - \xi^{(k)})u_{(k-1)} + \frac{1}{2}(1 + \xi^{(k)})u_{(k)}, \\ \phi_y^{(k)} &\equiv \frac{1}{2}(1 - \xi^{(k)})v_{(k-1)} + \frac{1}{2}(1 + \xi^{(k)})v_{(k)}, \end{aligned} \quad (3)$$

where  $\xi^{(k)}$  is the local dimensionless coordinate system in a  $k$ th layer, which can be defined

$$\xi^{(k)} = \frac{z - z_{(k-1)}}{h^{(k)}} - 1, \quad -1 < \xi^{(k)} < 1. \quad (4)$$

The interlaminar displacements are denoted by  $s_i$  ( $s = u, v; i = k, k-1$ ) and zero for the top and bottom layers:

$$u_{(0)} = u_{(N)} = v_{(0)} = v_{(N)} = 0. \quad (5)$$

Other interlaminar displacements fields are obtained by using a partial continuity of the shear stresses in the thickness direction of the composite plate [20]. The von Kármán strains [18], which take into account moderately large deflections and small strains in a  $k$  th layer, associated with the displacement field defined by modified zig-zag functions, can be expressed in the following form:

$$\begin{aligned} \varepsilon^{(k)} &= A + zB + \phi^{(k)}D + \chi, \\ \gamma^{(k)} &= R + F^{(k)}\psi, \end{aligned} \quad (6)$$

in which

$$\begin{aligned} \varepsilon^{(k)} &= \begin{bmatrix} \varepsilon_{xx}^{(k)} \\ \varepsilon_{yy}^{(k)} \\ \gamma_{xy}^{(k)} \end{bmatrix}, \quad A = \begin{bmatrix} u_{0,x} \\ v_{0,y} \\ u_{0,y} + v_{0,x} \end{bmatrix}, \quad B = \begin{bmatrix} \theta_{x,x} \\ \theta_{y,y} \\ \theta_{x,y} + \theta_{y,x} \end{bmatrix}, \quad D = \begin{bmatrix} \psi_{x,x} \\ \psi_{y,y} \\ \psi_{x,y} \\ \psi_{y,x} \end{bmatrix}, \\ \phi^{(k)} &= \begin{bmatrix} \phi_x^k & 0 & 0 & 0 \\ 0 & \phi_y^k & 0 & 0 \\ 0 & 0 & \phi_x^k & \phi_y^k \end{bmatrix}, \quad \chi = \begin{bmatrix} \frac{1}{2}w_{0,x}^2 \\ \frac{1}{2}w_{0,y}^2 \\ w_{0,x}w_{0,y} \end{bmatrix}, \quad \gamma^{(k)} = \begin{bmatrix} \gamma_{xz}^{(k)} \\ \gamma_{yz}^{(k)} \end{bmatrix}, \\ R &= \begin{bmatrix} w_{0,x} + \theta_x \\ w_{0,y} + \theta_y \end{bmatrix}, \quad \psi = \begin{bmatrix} \psi_x \\ \psi_y \end{bmatrix}, \quad F^{(k)} = \begin{bmatrix} \frac{\partial \phi_x^{(k)}(z)}{\partial z} & 0 \\ 0 & \frac{\partial \phi_y^{(k)}(z)}{\partial z} \end{bmatrix}, \end{aligned} \quad (7)$$

where  $(\odot)_{,\alpha} \equiv \frac{\partial(\odot)}{\partial \alpha}$  ( $\alpha = x, y$ ) is the partial derivative with respect to the midplane coordinate. In Eq. (6),  $\chi$  is a nonlinear term. Since the zig-zag functions  $\phi$  are the linear functions of  $z$  in each layer (i.e.,  $\frac{\partial \phi_x^{(k)}(z)}{\partial z} = cte$ ) and vanish in the upper ( $z = h$ ) and bottom ( $z = -h$ ) face, we conclude that

$$\int_{-h}^h \left\{ \frac{\partial \phi_x^{(k)}(z)}{\partial z}, \frac{\partial \phi_y^{(k)}(z)}{\partial z} \right\} dz = \sum_{k=1}^N 2h^{(k)} \left\{ \frac{\partial \phi_x^{(k)}(z)}{\partial z}, \frac{\partial \phi_y^{(k)}(z)}{\partial z} \right\} = 0. \quad (8)$$

Integrating Eq. (6) across the plate thickness and using Eq. (8), we found that

$$R = \frac{1}{2h} \int_{-h}^h \gamma^{(k)} dz. \quad (9)$$

Equation (9) indicates that the shear strains have two parts. One of them is the average shear angle, which is the same as the shear strain in the FSDT, and the other part includes the interlaminar effects expressed by zig-zag terms. According to the constitutive relations,

$$\begin{aligned} \sigma^{(k)} &= C^{(k)} \varepsilon^{(k)}, \\ \tau^{(k)} &= Q^{(k)} \gamma^{(k)}, \end{aligned} \quad (10)$$

where  $\sigma^{(k)}$  and  $\tau^{(k)}$  are the stresses;  $C^{(k)}$  and  $Q^{(k)}$  are the reduced stiffness coefficients relative to the in-plane condition. They are defined as

$$\sigma^{(k)} = \begin{pmatrix} \sigma_{xx} \\ \sigma_{yy} \\ \tau_{xy} \end{pmatrix}^{(k)}, \quad \tau^{(k)} = \begin{pmatrix} \tau_{xz} \\ \tau_{yz} \end{pmatrix}^{(k)}, \quad C^{(k)} = \begin{pmatrix} C_{11} & C_{12} & C_{16} \\ C_{12} & C_{22} & C_{26} \\ C_{16} & C_{26} & C_{66} \end{pmatrix}^{(k)}, \quad Q^{(k)} = \begin{pmatrix} Q_{11} & Q_{12} \\ Q_{12} & Q_{22} \end{pmatrix}^{(k)}. \quad (11)$$

Tessler et al. I [21] determined such zig-zag functions that the partial continuity of transvers shear stresses satisfied the following zig-zag functions:

$$\begin{cases} \phi_x^{(1)} = (z+h)\left(\frac{G_1}{Q_{11}^{(1)}} - 1\right), \\ \phi_y^{(1)} = (z+h)\left(\frac{G_2}{Q_{22}^{(1)}} - 1\right), \\ \phi_x^{(k)} = (z+h)\left(\frac{G_1}{Q_{11}^{(k)}} - 1\right) + \sum_{i=2}^k 2h^{(i-1)}\left(\frac{G_1}{Q_{11}^{(i-1)}} - \frac{G_1}{Q_{11}^{(k)}}\right) \quad (k=2,3,\dots,N), \\ \phi_y^{(k)} = (z+h)\left(\frac{G_2}{Q_{22}^{(k)}} - 1\right) + \sum_{i=2}^k 2h^{(i-1)}\left(\frac{G_2}{Q_{22}^{(i-1)}} - \frac{G_2}{Q_{22}^{(k)}}\right) \quad (k=2,3,\dots,N). \end{cases} \quad (12)$$

$G_1$  and  $G_2$  in Eq. (12) are the weighted-average transverse-shear coefficients, which are calculated by imposing constraint conditions on the zig-zag functions and are express as

$$\begin{cases} G_1 \\ G_2 \end{cases} = \begin{cases} \left(\frac{1}{h} \sum_{k=1}^N \frac{h^{(k)}}{Q_{11}^{(k)}}\right)^{-1} \\ \left(\frac{1}{h} \sum_{k=1}^N \frac{h^{(k)}}{Q_{22}^{(k)}}\right)^{-1} \end{cases}. \quad (13)$$

It is obvious from Eqs. (12), (13) that the zig-zag functions do not depend on the strain state and are determined by interlaminar properties.

### 3. Governing Equations

In this Section, the governing equations for a stress analysis of composite plates are derived. According to the principle of virtual work, if a particle is in equilibrium, the total virtual work of forces acting on the particle is zero for any virtual displacement. Using this principle, the governing equations are obtained. Consider a composite plate subjected to a transverse force  $q(x, y)$ , i.e.,

$$\int_A \int_{-h}^h (\sigma^{(k)T} \delta \varepsilon^{(k)} + \tau^{(k)T} \delta \gamma^{(k)}) dz dA - \int_A q \delta w dA = 0, \quad (14)$$

where  $A(z=0)$  is the midplane area of the composite plate and  $\delta$  is the variation operator. The transverse force remains perpendicular to the plate midsurface, and the local direction (i.e., to the normal surface) of the midsurface remains in the  $z$  direction. Inserting Eqs. (6) and (10) into (14), we obtain that

$$\begin{aligned} & \int_A \{ (N_x \delta u_{0,x} + M_x \delta \theta_{x,x} + M_x^\phi \delta \psi_{x,x} + w_{,x} \delta w_{,x} N_x) \\ & + (N_y \delta v_{0,y} + M_y \delta \theta_{y,y} + M_y^\phi \delta \psi_{y,y} + w_{0,y} \delta w_{0,y} N_y) \} \end{aligned}$$

$$\begin{aligned}
& +[N_{xy}(\delta u_{0,y} + \delta v_{0,x}) + M_{xy}(\delta \theta_{x,y} + \delta \theta_{y,x}) + M_{xy}^\phi \delta \psi_{x,y} \\
& + M_{yx}^\phi \delta \psi_{y,x} + \delta w_{0,x} w_{0,y} N_{xy} + w_{0,x} \delta w_{0,y} N_{xy}] , \\
Q_x(\delta w_{0,x} + \delta \theta_x) + Q_x^\phi \delta \psi_x + Q_y(\delta w_{0,y} + \delta \theta_y) + Q_y^\phi \delta \psi_y - q \delta w \} dA = 0 ,
\end{aligned} \tag{15}$$

where  $N$  and  $M$  are the resultants of the membrane and bending stresses, respectively, and  $Q$  is the resultant of the transverse shear stresses,

$$\begin{aligned}
N_m^T & \equiv \{N_x, N_y, N_{xy}\} = \int_{-h}^h \{\sigma_{xx}^{(k)}, \sigma_{yy}^{(k)}, \sigma_{xy}^{(k)}\} dz , \\
M_m^T & \equiv \{M_x, M_x^\phi, M_y, M_y^\phi, M_{xy}, M_{xy}^\phi, M_{yx}^\phi\} \\
& = \int_{-h}^h \{z \sigma_{xx}^{(k)}, \phi_x^{(k)} \sigma_{xx}^{(k)}, z \sigma_{yy}^{(k)}, \phi_y^{(k)} \sigma_{yy}^{(k)}, z \tau_{xy}^{(k)}, \phi_x^{(k)} \tau_{xy}^{(k)}, \phi_y^{(k)} \tau_{xy}^{(k)}\} dz , \\
Q_s^T & \equiv \{Q_y, Q_y^\phi, Q_x, Q_x^\phi\} = \int_{-h}^h \{\tau_{yz}^{(k)}, \frac{\partial \phi_y^{(k)}(z)}{\partial z} \tau_{yz}^{(k)}, \tau_{xz}^{(k)}, \frac{\partial \phi_x^{(k)}(z)}{\partial z} \tau_{xz}^{(k)}\} dz .
\end{aligned} \tag{16}$$

Integrating Eq. (14) by parts, we have

$$\begin{aligned}
& -\int_A N_{x,x} \delta u_0 dA - \int_A M_{x,x} \delta \theta_x dA - \int_A M_{x,x}^\phi \delta \psi_x dA + \int_A (N_x w_{0,x})_{,x} \delta w_0 dA \\
& -\int_A N_{y,y} \delta v_0 dA - \int_A M_{y,y} \delta \theta_y dA - \int_A M_{y,y}^\phi \delta \psi_y dA - \int_A (N_y w_{0,y})_{,y} \delta w_0 dA \\
& -\int_A N_{xy,y} \delta u_0 dA + \int_A N_{xy,x} \delta v_0 dA - \int_A M_{xy,y} \delta \theta_x dA - \int_A M_{xy,x} \delta \theta_y dA \\
& -\int_A M_{xy,y}^\phi \delta \psi_x dA - \int_A M_{yx,x}^\phi \delta \psi_y dA - \int_A (N_{xy} w_{0,y})_{,x} \delta w_0 dA \\
& -\int_A (N_{xy} w_{0,x})_{,y} \delta w_0 dA - \int_A Q_{x,x} \delta w_0 dA + \int_A Q_x \delta \theta_x dA + \int_A Q_x^\phi \delta \psi_x dA \\
& -\int_A Q_{y,y} \delta w_0 dA + \int_A Q_y \delta \theta_y dA + \int_A Q_y^\phi \delta \psi_y dA - \int_A q \delta w_0 dA + B.C. \} dA = 0 ,
\end{aligned} \tag{17}$$

where  $B.C.$  are the terms of the boundary condition of the plate. By simplifying Eq. (17), the following governing equations are found (the extended form of these equations, in terms of displacements is given in the appendix A):

$$\begin{cases}
\delta u_0 : N_{x,x} + N_{xy,y} = 0 \\
\delta v_0 : N_{y,y} + N_{xy,x} = 0 \\
\delta w_0 : Q_{x,x} + Q_{y,y} + q - N(w) = 0 \\
\delta \theta_x : M_{x,x} + M_{xy,y} = Q_x \\
\delta \theta_y : M_{y,y} + M_{xy,x} = Q_y \\
\delta \psi_x : M_{x,x}^\phi + M_{xy,y}^\phi = Q_x^\phi \\
\delta \psi_y : M_{y,y}^\phi + M_{yx,x}^\phi = Q_y^\phi
\end{cases} , \tag{18}$$

where  $N(w)$  is a nonlinear term that is included in (18) to take into account the nonlinear strains and is defined as

$$N(w) \equiv \frac{\partial}{\partial x} (N_x \frac{\partial w_0}{\partial x} + N_{xy} \frac{\partial w_0}{\partial y}) + \frac{\partial}{\partial y} (N_y \frac{\partial w_0}{\partial y} + N_{xy} \frac{\partial w_0}{\partial x}) . \tag{19}$$

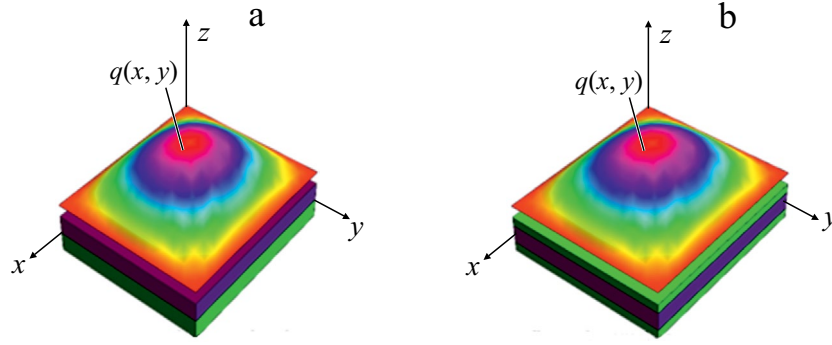


Fig. 2. Two- (a) and three-layered (b) composite plates.

#### 4. Solution Procedure

Let us consider a rectangular composite plate of length  $a$  and width  $b$ , and thickness  $2h$  consisting of  $N$  layers, as shown in Fig. 2. The plate is simply supported:

$$\begin{cases} y = 0, b, 0 < x < a \rightarrow v_0 = w_0 = \theta_y = \psi_y = N_x = M_x = M_x^\phi = 0, \\ x = 0, a, 0 < y < b \rightarrow u_0 = w_0 = \theta_x = \psi_x = N_y = M_y = M_y^\phi = 0. \end{cases} \quad (20)$$

Using the Galerkin approach, the kinematic unknowns that satisfy boundary conditions (20) are expressed in the following form:

$$\begin{aligned} u_0 &= \sum_{m=1}^{\infty} \sum_{n=1}^{\infty} U_{mn} \cos \frac{n\pi x}{a} \sin \frac{m\pi y}{b}, \\ \theta_x &= \sum_{m=1}^{\infty} \sum_{n=1}^{\infty} \Theta x_{mn} \cos \frac{n\pi x}{a} \sin \frac{m\pi y}{b}, \\ \psi_x &= \sum_{m=1}^{\infty} \sum_{n=1}^{\infty} \Psi x_{mn} \cos \frac{n\pi x}{a} \sin \frac{m\pi y}{b}, \\ v_0 &= \sum_{m=1}^{\infty} \sum_{n=1}^{\infty} V_{mn} \sin \frac{n\pi x}{a} \cos \frac{m\pi y}{b}, \\ \theta_y &= \sum_{m=1}^{\infty} \sum_{n=1}^{\infty} \Theta y_{mn} \sin \frac{n\pi x}{a} \cos \frac{m\pi y}{b}, \\ \psi_y &= \sum_{m=1}^{\infty} \sum_{n=1}^{\infty} \Psi y_{mn} \sin \frac{n\pi x}{a} \cos \frac{m\pi y}{b}, \\ w_0 &= \sum_{m=1}^{\infty} \sum_{n=1}^{\infty} W_{mn} \sin \frac{n\pi x}{a} \sin \frac{m\pi y}{b}, \end{aligned} \quad (21)$$

where  $U_{mn}, V_{mn}, W_{mn}, \Theta x_{mn}, \Theta y_{mn}, \psi y_{mn}$ , and  $\psi x_{mn}$  are unknown coefficients, which are calculated by governing equations (18). The system of differential equations (18) is reduced to a system of algebraic equations, which is solved to obtain the unknown coefficients of Eq. (21). The distribution of the transverse loads  $q(x, y)$  is assumed sinusoidal:

$$q(x, y) = q_0 \sin \frac{\pi x}{a} \sin \frac{\pi y}{b} = \sum_{m=1}^{\infty} \sum_{n=1}^{\infty} q_{mn} \sin \frac{n\pi x}{a} \sin \frac{m\pi y}{b}. \quad (22)$$

TABLE 1. Mechanical Properties of Layers Materials

Property	Orthotropic layer (carbon fibers and epoxy)	Isotropic layer (polymer)
$E_1$	157.9 GPa	0.1040 GPa
$E_2=E_3$	9.584 GPa	0.1040 GPa
$\nu_{23}$	0.49	0.3
$\nu_{13} = \nu_{12}$	0.32	0.3
$G_{23}$	3.227 GPa	0.04 GPa
$G_{13} = G_{12}$	5.930 GPa	0.04 GPa

TABLE 2. Layer Construction of Each Plate

Plate type	Composite plate with two layers	Sandwich panel with three layers
Layer material	C–C	C–P–C
Fiber orientation	0/90	0/0/0
Layer thickness	0.5–0.5	0.1–0.8–0.1

## 5. Results and Discussion

As shown in the previous Section, the geometric nonlinearities are taken into account in our investigation of two- and three-layered composite plates. The mechanical properties of their layers are listed in Table 1, and the layout of each plate is illustrated in Table 2 and Fig. 2. The numerical results obtained were compared with those available in the literature, including results of the refined zig-zag theory (RZT) [21], the exact of Pagano solution [34], and results of the first-order shear-deformation theory (FSDT). The number of adequate terms ( $n = m = 30$ ) was obtained by a convergence analysis of Eqs. (21), where the maximum transverse displacement was considered. The FSDT results are presented considering the non-linearity effect, but there is no nonlinearity in the RZT and the elasticity Pagano solution. Therefore, the NRZT (nonlinear refined zig-zag theory) is compared with RZT and the nonlinear FSDT. The RZT is also compared with the Pagano solution to show the capability of RZT. The main difference between the RZT and ZT (Di Sciuva zig-zag theory) is that the zig-zag function is eliminated only from the outer surfaces of the laminated beam, but not from layers. This important difference ensures a more physically realistic distribution of the zig-zag function — it is nonzero across the plate depth, and, as a result, the new zig-zag function ensures a contribution from each layer to the overall deformation. The dimensionless mechanical parameters are defined in the following form:

$$\begin{aligned}
 \bar{u} &\equiv \frac{10^4 D_{11}}{q_0 a^4} u^{(k)}\left(a, \frac{b}{2}, z\right), \\
 \bar{\sigma}_{xx} &\equiv \frac{(2h)^2}{q_0 a^2} \sigma_{xx}^{(k)}\left(\frac{a}{2}, \frac{b}{2}, z\right), \\
 \bar{\tau}_{xz} &\equiv \frac{(2h)}{q_0 a} \tau_{xz}^{(k)}\left(0, \frac{b}{2}, z\right), \\
 \bar{w} &= \frac{100 D_{11}}{q_0 a^4} w\left(\frac{a}{2}, \frac{b}{2}\right).
 \end{aligned} \tag{23}$$

A systematic study was performed to show the reliability and accuracy of the presented model. Figure 3 depicts the dimensionless in-plane displacements of two- and three-layered composite plates in the  $x$  direction based on various



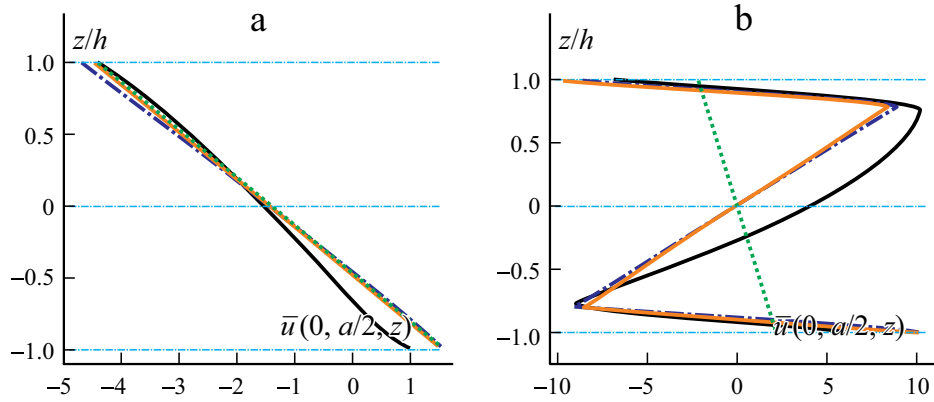


Fig. 3. Dimensionless in-plane displacement  $\bar{u}$  across the thickness  $z/h$  of two- (a) and three-layered (b) plates according to various theories.

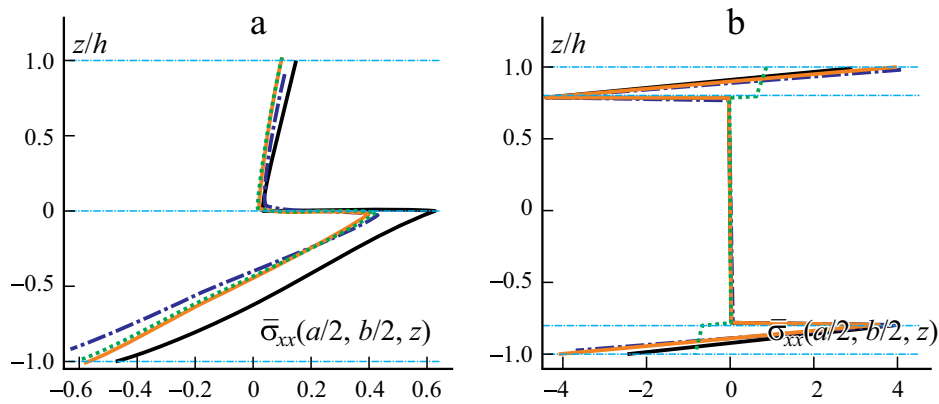


Fig. 4. Dimensionless in-plane stress  $\bar{\sigma}$  across the thickness  $z/h$  of two- (a) and three-layered (b) plates according to various theories.

models. The presented model (NRZT) and the RZT close together, especially in the linear regions. The difference between them increases in nonlinear problems when the load increases. These results could be closer to the exact solution if higher-order functions were chosen as the zig-zag function. Figure 3b clearly exhibits the superiority of the current model over the FSDT. As shown, the FSDT estimates the entire displacement field only by one continuous function, but the current model employs a continuous function for each layer. This dissimilarity in predicting displacement functions causes the major difference in the numerical results, particularly for composite plates with a greater number of layers.

Figure 4 shows variations in the in-plane stress parameter in terms of the  $z$  coordinate at the center of two- and three-layered composite plates in different theories. What stands out from the figures mentioned is that the model implemented gives a better accuracy than the FSDT. Looking at the curves associated with the FSDT, it can be concluded that the FSDT underestimates the in-plane stresses, particularly on the boundary planes, where the highest tension and compression take place even though a shear correction factor is used. In this theory, a linear distribution is used for the transverse shear stresses across the thickness of the structure. In the present theory, piecewise constant stresses are taken into account, which reduces errors in the global response of the sandwich structure. What is more, the figures plotted imply that the consideration of geometric nonlinearities yields lower normal stresses, especially for face sheets.

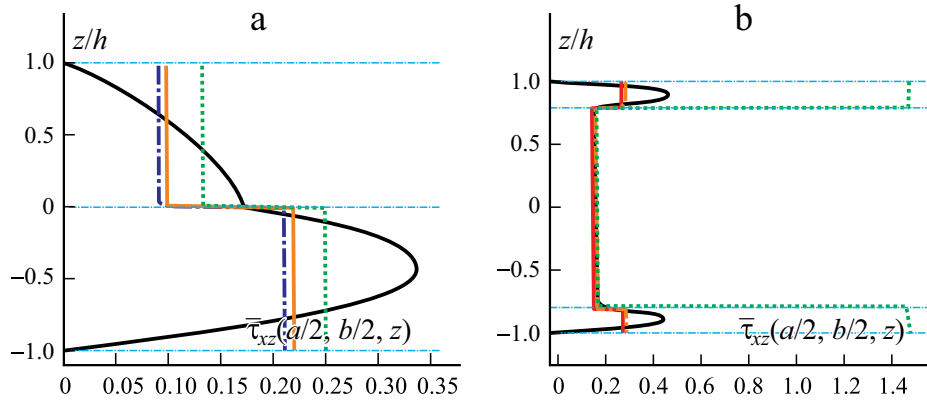


Fig. 5. Dimensionless transverse shear stress  $\bar{\tau}_{xz}$  across the thickness  $z/h$  of two- (a) and three-layered (b) plates according to various theories.

TABLE 3. Dimensionless Out-of-Plane Displacements in Different Theories of Sandwich Plates

$a/2h$	Exact	FSDT	Zig-zag (Di Sciuva)	Refined Zig-zag theory (RZT)	Present (NRZT)
4	42.420	3.739	42.124	42.189	42.480
10	9.734	1.321	9.738	9.739	9.737
20	3.487	0.948	3.489	3.490	3.488
50	1.305	0.841	1.305	1.305	1.305
100	0.945	0.826	0.945	0.945	0.945
200	0.852	0.822	0.852	0.852	0.852

Figure 5 demonstrates variations in the transverse shear stress parameter at the center of two- and three-layered composite plates for different models across the thickness. It can be seen that, although the presented model predicts a constant shear strain for each layer, the numerical results are in a better agreement with those given by the exact solution. In fact, the continuity of shear stresses not fulfilled in such modified zig-zag theory as the FSDT, but considering a layerwise function for each layer, makes the results found are closer to the exact solution. This fact is far more pronounced in the face sheets, as the FSDT anticipates the transverse shear stress with errors more than 60 percent, while the current model gives a better estimate for stresses in comparison with the 3D elasticity solution. In addition, it is seen that excluding nonlinear strains leads to higher shear strains. The distribution of shear stresses could be changed by choosing a higher-order zig-zag function.

The dimensionless out-of-plane displacements of the sandwich considered plate at its center according to various theories is listed in Table 3. On increasing the thickness ratio, all models approach the same accuracy. This is because the effects of shear strains can be ignored for structures with a low thickness-to-span ratio. In addition, as is seen, the nonlinear effects increased the stiffness of the sandwich plate and, as a result, the deflections found considering the nonlinearity are smaller than for the other models.

Figure 6 depicts the impacts of load density on the central deflection of a three-layer composite plate. As is seen, the inclusion of geometric nonlinearities is more notable for larger values of load intensity. This is due to the fact that the structure withstands more deformations when it is subjected to a higher loading. Furthermore, it is observed that the difference between the linear and nonlinear theories is more pronounced in a rectangular plate ( $R = 0.5$ ) than in a square one ( $R = 1$ ), which indicates that the inclusion of geometric nonlinearity makes their deformation more sensitive to the aspect ratio.

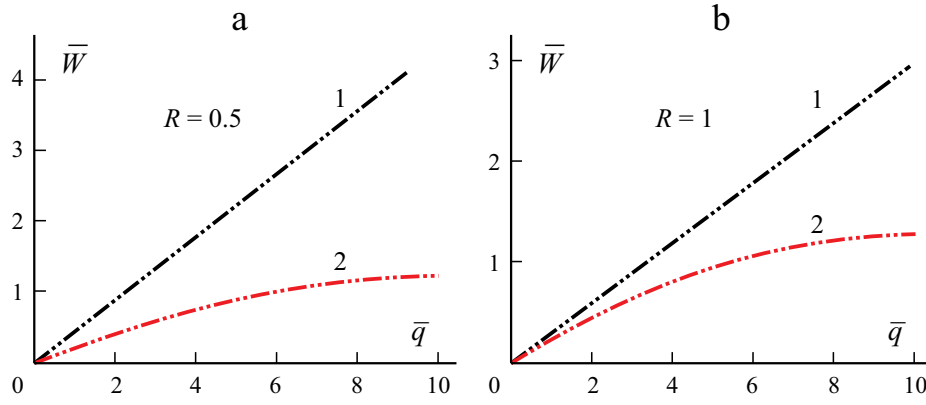


Fig. 6. Variations in the deflection parameter  $\bar{w}$  vs. the load intensity parameter  $\bar{q}$  for rectangular ( $R = 0.5$ ) (a) and square ( $R = 1$ ) (b) plates.

## Conclusion

In the present work, a static analysis of composite plates was carried out using the zig-zag theory. In order to consider large strain, nonlinear von Kármán strains were considered. The displacement field was estimated using the first-order shear-deformation theory. Modified linear zig-zag functions were taken into account in order to improve the shear stresses and the interlaminar behavior of the plates. These linear functions depend on layer properties and are obtained for each layer separately. In contrast to the FSDT, this theory does not need any shear correction factor. The governing and kinematic equations not depend on the number of layers. This advantage to a simplicity and reduces the computational time. Numerical results for a laminated simply supported composite plate are presented to show the effect of geometric nonlinearity. These results are compared with results of the FSDT and the 3D elasticity solution, and they show a high accuracy of the current work. The FSDT estimates the entire displacement field only with one continuous function while the current model uses a continuous function for each layer. On increasing the thickness-to-span ratio, all models approach the same accuracy. This is due to the fact that the effects of shear strain can be ignored for structures with a low thickness-to-span ratio. Choosing a higher-order function as the zig-zag function more accurate results can be reached. The model proposed gives high-accuracy results for nonlinear problems.

## Appendix A: Governing Equations in Terms of Displacements

Equations (18) can be expanded as follows.

$$\begin{aligned}
& T_{11} \left( \frac{\partial^2 u_0}{\partial x^2} + \frac{\partial w_0}{\partial x} \frac{\partial^2 w_0}{\partial x^2} \right) + T_{12} \left( \frac{\partial^2 v_0}{\partial y \partial x} + \frac{\partial w_0}{\partial y} \frac{\partial^2 w_0}{\partial x \partial y} \right) + T_{16} \left( 2 \frac{\partial^2 u_0}{\partial x \partial y} + \frac{\partial^2 v_0}{\partial x^2} + \frac{\partial w_0}{\partial y} \frac{\partial^2 w_0}{\partial x^2} \right) \\
& + 2T_{16} \left( \frac{\partial w_0}{\partial x} \frac{\partial^2 w_0}{\partial x \partial y} \right) + T_{26} \left( \frac{\partial^2 v_0}{\partial y^2} + \frac{\partial w_0}{\partial y} \frac{\partial^2 w_0}{\partial y^2} \right) + T_{66} \left( \frac{\partial^2 u_0}{\partial y^2} + \frac{\partial^2 v_0}{\partial x \partial y} + \frac{\partial w_0}{\partial y} \frac{\partial^2 w_0}{\partial x \partial y} + \frac{\partial w_0}{\partial x} \frac{\partial^2 w_0}{\partial y^2} \right) \\
& + S_{11} \frac{\partial^2 \theta_x}{\partial x^2} + S_{12} \frac{\partial^2 \theta_y}{\partial y \partial x} + S_{16} \left( 2 \frac{\partial^2 \theta_x}{\partial x \partial y} + \frac{\partial^2 \theta_y}{\partial x^2} \right) + S_{26} \frac{\partial^2 \theta_y}{\partial y^2} + S_{66} \left( \frac{\partial^2 \theta_x}{\partial y^2} + \frac{\partial^2 \theta_y}{\partial x \partial y} \right) \\
& + L_{11x} \frac{\partial^2 \psi_x}{\partial x^2} + L_{12y} \frac{\partial^2 \psi_y}{\partial y \partial x} + 2L_{16x} \frac{\partial^2 \psi_x}{\partial x \partial y} + L_{16y} \frac{\partial^2 \psi_y}{\partial x^2} + L_{26y} \frac{\partial^2 \psi_y}{\partial y^2} + L_{66x} \frac{\partial^2 \psi_x}{\partial y^2} + L_{66y} \frac{\partial^2 \psi_y}{\partial x \partial y} = 0, \quad (\text{A-1})
\end{aligned}$$

$$\begin{aligned}
& T_{22}(\frac{\partial^2 v_0}{\partial y^2} + \frac{\partial w_0}{\partial y} \frac{\partial^2 w_0}{\partial y^2}) + T_{12}(\frac{\partial^2 u_0}{\partial x \partial y} + \frac{\partial w_0}{\partial x} \frac{\partial^2 w_0}{\partial x \partial y}) + T_{16}(\frac{\partial^2 u_0}{\partial x^2} + \frac{\partial w_0}{\partial x} \frac{\partial^2 w_0}{\partial x^2}) \\
& + T_{26}(\frac{\partial^2 u_0}{\partial y^2} + 2 \frac{\partial^2 v_0}{\partial x \partial y} + 2 \frac{\partial w_0}{\partial y} \frac{\partial^2 w_0}{\partial x \partial y} + \frac{\partial w_0}{\partial x} \frac{\partial^2 w_0}{\partial y^2}) + T_{66}(\frac{\partial^2 u_0}{\partial y \partial x} + \frac{\partial^2 v_0}{\partial x^2} + \frac{\partial w_0}{\partial y} \frac{\partial^2 w_0}{\partial x^2}) \\
& + T_{66}(\frac{\partial w_0}{\partial x} \frac{\partial^2 w_0}{\partial y \partial x}) + S_{12} \frac{\partial^2 \theta_x}{\partial x \partial y} + S_{22} \frac{\partial^2 \theta_y}{\partial y^2} + S_{26}(\frac{\partial^2 \theta_x}{\partial y^2} + 2 \frac{\partial^2 \theta_y}{\partial x \partial y}) + S_{16} \frac{\partial^2 \theta_x}{\partial x^2} + S_{66}(\frac{\partial^2 \theta_x}{\partial y \partial x} + \frac{\partial^2 \theta_y}{\partial x^2}) \\
& + L_{12x} \frac{\partial^2 \psi_x}{\partial x \partial y} + L_{16x} \frac{\partial^2 \psi_x}{\partial x^2} + L_{22y} \frac{\partial^2 \psi_y}{\partial y^2} + L_{26x} \frac{\partial^2 \psi_x}{\partial y^2} + 2L_{26y} \frac{\partial^2 \psi_y}{\partial x \partial y} + L_{66x} \frac{\partial^2 \psi_x}{\partial y \partial x} + L_{66y} \frac{\partial^2 \psi_y}{\partial x^2} = 0, \quad (A-2)
\end{aligned}$$

$$\begin{aligned}
& F_{12}(2 \frac{\partial^2 w_0}{\partial x \partial y} + \frac{\partial \theta_y}{\partial x} + \frac{\partial \theta_x}{\partial y}) + F_{11}(\frac{\partial^2 w_0}{\partial x^2} + \frac{\partial \theta_x}{\partial x}) + F_{22}(\frac{\partial^2 w_0}{\partial y^2} + \frac{\partial \theta_y}{\partial y}) \\
& + E_{11x} \frac{\partial \psi_x}{\partial x} + E_{22y} \frac{\partial \psi_y}{\partial y} + E_{12x} \frac{\partial \psi_x}{\partial y} + E_{12y} \frac{\partial \psi_y}{\partial x} + q - N(w) = 0, \quad (A-3)
\end{aligned}$$

$$\begin{aligned}
& S_{11}(\frac{\partial^2 u_0}{\partial x^2} + \frac{\partial w_0}{\partial x} \frac{\partial^2 w_0}{\partial x^2}) + S_{12}(\frac{\partial^2 v_0}{\partial y \partial x} + \frac{\partial w_0}{\partial y} \frac{\partial^2 w_0}{\partial y \partial x}) + S_{16}(\frac{\partial^2 u_0}{\partial y \partial x} + \frac{\partial^2 v_0}{\partial x^2} + \frac{\partial^2 w_0}{\partial x^2} \frac{\partial w_0}{\partial y}) \\
& + S_{16}(\frac{\partial^2 u_0}{\partial x \partial y} + \frac{\partial w_0}{\partial x} \frac{\partial^2 w_0}{\partial x \partial y} + \frac{\partial w_0}{\partial x} \frac{\partial^2 w_0}{\partial y \partial x}) + S_{66}(\frac{\partial^2 u_0}{\partial y^2} + \frac{\partial^2 v_0}{\partial x \partial y} + \frac{\partial^2 w_0}{\partial x \partial y} \frac{\partial w_0}{\partial y} + \frac{\partial w_0}{\partial x} \frac{\partial^2 w_0}{\partial y^2}) \\
& + S_{26}(\frac{\partial^2 v_0}{\partial y^2} + \frac{\partial w_0}{\partial y} \frac{\partial^2 w_0}{\partial y^2}) + J_{11} \frac{\partial^2 \theta_x}{\partial x^2} + J_{12} \frac{\partial^2 \theta_y}{\partial y \partial x} + J_{16}(\frac{\partial^2 \theta_x}{\partial y \partial x} + \frac{\partial^2 \theta_y}{\partial x^2}) + J_{26} \frac{\partial^2 \theta_y}{\partial y^2} + J_{16} \frac{\partial^2 \theta_x}{\partial x \partial y} \\
& + J_{66}(\frac{\partial^2 \theta_x}{\partial y^2} + \frac{\partial^2 \theta_y}{\partial x \partial y}) + K_{16x} \frac{\partial^2 \psi_x}{\partial y \partial x} + K_{16y} \frac{\partial^2 \psi_y}{\partial x^2} + K_{11x} \frac{\partial^2 \psi_x}{\partial x^2} + K_{12y} \frac{\partial^2 \psi_y}{\partial y \partial x} + K_{16x} \frac{\partial^2 \psi_x}{\partial x \partial y} + K_{26y} \frac{\partial^2 \psi_y}{\partial y^2} \\
& + K_{66x} \frac{\partial^2 \psi_x}{\partial y^2} + K_{66y} \frac{\partial^2 \psi_y}{\partial x \partial y} = F_{12}(\frac{\partial w_0}{\partial y} + \theta_y) + E_{12y} \psi_y + F_{11}(\frac{\partial w_0}{\partial x} + \theta_x) + E_{11x} \psi_x = 0, \quad (A-4)
\end{aligned}$$

$$\begin{aligned}
& S_{12}(\frac{\partial^2 u_0}{\partial x \partial y} + \frac{\partial w_0}{\partial x} \frac{\partial^2 w_0}{\partial x \partial y}) + S_{22}(\frac{\partial^2 v_0}{\partial y^2} + \frac{\partial w_0}{\partial y} \frac{\partial^2 w_0}{\partial y^2}) + S_{26}(\frac{\partial^2 u_0}{\partial y^2} + \frac{\partial^2 v_0}{\partial x \partial y} + \frac{\partial^2 w_0}{\partial x \partial y} \frac{\partial w_0}{\partial y}) \\
& + S_{26}(\frac{\partial^2 v_0}{\partial y \partial x} + \frac{\partial w_0}{\partial y} \frac{\partial^2 w_0}{\partial y \partial x} + \frac{\partial w_0}{\partial x} \frac{\partial^2 w_0}{\partial y^2}) + S_{66}(\frac{\partial^2 u_0}{\partial y \partial x} + \frac{\partial^2 v_0}{\partial x^2} + \frac{\partial^2 w_0}{\partial x^2} \frac{\partial w_0}{\partial y} + \frac{\partial w_0}{\partial x} \frac{\partial^2 w_0}{\partial y \partial x}) \\
& + S_{16}(\frac{\partial^2 u_0}{\partial x^2} + \frac{\partial w_0}{\partial x} \frac{\partial^2 w_0}{\partial x^2}) + J_{12} \frac{\partial^2 \theta_x}{\partial x \partial y} + J_{22} \frac{\partial^2 \theta_y}{\partial y^2} + J_{26}(\frac{\partial^2 \theta_x}{\partial y^2} + \frac{\partial^2 \theta_y}{\partial x \partial y}) + J_{16} \frac{\partial^2 \theta_x}{\partial x^2} + J_{26} \frac{\partial^2 \theta_y}{\partial y \partial x} \\
& + J_{66}(\frac{\partial^2 \theta_x}{\partial y \partial x} + \frac{\partial^2 \theta_y}{\partial x^2}) + K_{26x} \frac{\partial^2 \psi_x}{\partial y^2} + K_{26y} \frac{\partial^2 \psi_y}{\partial x \partial y} + K_{12x} \frac{\partial^2 \psi_x}{\partial x \partial y} + K_{22y} \frac{\partial^2 \psi_y}{\partial y^2} + K_{16x} \frac{\partial^2 \psi_x}{\partial x^2} + K_{26y} \frac{\partial^2 \psi_y}{\partial y \partial x} \\
& + K_{66x} \frac{\partial^2 \psi_x}{\partial y \partial x} + K_{66y} \frac{\partial^2 \psi_y}{\partial x^2} = F_{22}(\frac{\partial w_0}{\partial y} + \theta_y) + E_{22y} \psi_y + F_{12}(\frac{\partial w_0}{\partial x} + \theta_x) + E_{12x} \psi_x = 0, \quad (A-5)
\end{aligned}$$

$$L_{11x}(\frac{\partial^2 u_0}{\partial x^2} + \frac{\partial w_0}{\partial x} \frac{\partial^2 w_0}{\partial x^2}) + K_{11x} \frac{\partial^2 \theta_x}{\partial x^2} + H_{11xx} \frac{\partial^2 \psi_x}{\partial x^2} + L_{12x}(\frac{\partial^2 v_0}{\partial y \partial x} + \frac{\partial w_0}{\partial y} \frac{\partial^2 w_0}{\partial y \partial x}) + K_{12x} \frac{\partial^2 \theta_y}{\partial y \partial x}$$

$$\begin{aligned}
& +H_{12,yx} \frac{\partial^2 \psi_y}{\partial y \partial x} + L_{16,x} \left( \frac{\partial^2 u_0}{\partial y \partial x} + \frac{\partial^2 v_0}{\partial x^2} + \frac{\partial^2 w_0}{\partial x^2} \frac{\partial w_0}{\partial y} + \frac{\partial w_0}{\partial x} \frac{\partial^2 w_0}{\partial y \partial x} \right) + K_{16,x} \left( \frac{\partial^2 \theta_x}{\partial y \partial x} + \frac{\partial^2 \theta_y}{\partial x^2} \right) + H_{16,xx} \frac{\partial^2 \psi_x}{\partial y \partial x} \\
& + H_{16,yx} \frac{\partial^2 \psi_y}{\partial x^2} + L_{16,x} \left( \frac{\partial^2 u_0}{\partial x \partial y} + \frac{\partial w_0}{\partial x} \frac{\partial^2 w_0}{\partial x \partial y} \right) + K_{16,x} \frac{\partial^2 \theta_x}{\partial x \partial y} + H_{16,xx} \frac{\partial^2 \psi_x}{\partial x \partial y} + L_{26,x} \left( \frac{\partial^2 v_0}{\partial y^2} + \frac{\partial w_0}{\partial y} \frac{\partial^2 w_0}{\partial y^2} \right) \\
& + K_{26,x} \frac{\partial^2 \theta_y}{\partial y^2} + H_{26,xy} \frac{\partial^2 \psi_y}{\partial y^2} + L_{66,x} \left( \frac{\partial^2 u_0}{\partial y^2} + \frac{\partial^2 v_0}{\partial x \partial y} + \frac{\partial^2 w_0}{\partial x \partial y} \frac{\partial w_0}{\partial y} + \frac{\partial w_0}{\partial x} \frac{\partial^2 w_0}{\partial y^2} \right) + K_{66,x} \left( \frac{\partial^2 \theta_x}{\partial y^2} + \frac{\partial^2 \theta_y}{\partial x \partial y} \right) \\
& + H_{66,xx} \frac{\partial^2 \psi_x}{\partial y^2} + H_{66,xy} \frac{\partial^2 \psi_y}{\partial x \partial y} = E_{12,x} \left( \frac{\partial w_0}{\partial y} + \theta_y \right) + P_{12,yx} \psi_y + E_{11,x} \left( \frac{\partial w_0}{\partial x} + \theta_x \right) + P_{11,xx} \psi_x = 0, \tag{A-6}
\end{aligned}$$

$$\begin{aligned}
& L_{12,y} \left( \frac{\partial^2 u_0}{\partial x \partial y} + \frac{\partial w_0}{\partial x} \frac{\partial^2 w_0}{\partial x \partial y} \right) + K_{12,y} \frac{\partial^2 \theta_x}{\partial x \partial y} + H_{12,yx} \frac{\partial^2 \psi_x}{\partial x \partial y} + L_{22,y} \left( \frac{\partial^2 v_0}{\partial y^2} + \frac{\partial w_0}{\partial y} \frac{\partial^2 w_0}{\partial y^2} \right) + K_{22,y} \frac{\partial^2 \theta_y}{\partial y^2} \\
& + H_{22,yy} \frac{\partial^2 \psi_y}{\partial y^2} + L_{26,y} \left( \frac{\partial^2 u_0}{\partial y^2} + \frac{\partial^2 v_0}{\partial x \partial y} + \frac{\partial^2 w_0}{\partial x \partial y} \frac{\partial w_0}{\partial y} + \frac{\partial w_0}{\partial x} \frac{\partial^2 w_0}{\partial y^2} \right) + K_{26,y} \left( \frac{\partial^2 \theta_x}{\partial y^2} + \frac{\partial^2 \theta_y}{\partial x \partial y} \right) + L_{26,x} \frac{\partial^2 \psi_x}{\partial y^2} \\
& + H_{26,xy} \frac{\partial^2 \psi_y}{\partial x \partial y} + L_{16,y} \left( \frac{\partial^2 u_0}{\partial x^2} + \frac{\partial w_0}{\partial x} \frac{\partial^2 w_0}{\partial x^2} \right) + K_{16,y} \frac{\partial^2 \theta_x}{\partial x^2} + H_{16,yx} \frac{\partial^2 \psi_x}{\partial x^2} + L_{26,y} \left( \frac{\partial^2 v_0}{\partial y \partial x} + \frac{\partial w_0}{\partial y} \frac{\partial^2 w_0}{\partial y \partial x} \right) \\
& + K_{26,y} \frac{\partial^2 \theta_y}{\partial y \partial x} + H_{26,yy} \frac{\partial^2 \psi_y}{\partial y \partial x} + L_{66,y} \left( \frac{\partial^2 u_0}{\partial y \partial x} + \frac{\partial^2 v_0}{\partial x^2} + \frac{\partial^2 w_0}{\partial x^2} \frac{\partial w_0}{\partial y} + \frac{\partial w_0}{\partial x} \frac{\partial^2 w_0}{\partial y \partial x} \right) + K_{66,y} \left( \frac{\partial^2 \theta_x}{\partial y \partial x} + \frac{\partial^2 \theta_y}{\partial x^2} \right) \\
& + H_{66,xy} \frac{\partial^2 \psi_x}{\partial y \partial x} + H_{66,yy} \frac{\partial^2 \psi_y}{\partial x^2} = E_{22,y} \left( \frac{\partial w_0}{\partial y} + \theta_y \right) + P_{22,yy} \psi_y + E_{12,y} \left( \frac{\partial w_0}{\partial x} + \theta_x \right) + P_{12,yx} \psi_x = 0. \tag{A-7}
\end{aligned}$$

## Appendix B: Coefficients of Governing Equations

Coefficients utilized in Appendix A can be written as follows.

$$T_{11} = \int_{-h}^h C_{11}^{(k)} dz, T_{66} = \int_{-h}^h C_{66}^{(k)} dz, T_{12} = \int_{-h}^h C_{12}^{(k)} dz, \tag{B-1}$$

$$T_{22} = \int_{-h}^h C_{22}^{(k)} dz, T_{16} = \int_{-h}^h C_{16}^{(k)} dz, T_{26} = \int_{-h}^h C_{26}^{(k)} dz,$$

$$S_{11} = \int_{-h}^h C_{11}^{(k)} z dz, S_{66} = \int_{-h}^h C_{66}^{(k)} z dz, S_{16} = \int_{-h}^h C_{16}^{(k)} z dz, \tag{B-2}$$

$$S_{12} = \int_{-h}^h C_{12}^{(k)} z dz, S_{22} = \int_{-h}^h C_{22}^{(k)} z dz, S_{26} = \int_{-h}^h C_{26}^{(k)} z dz;$$

$$J_{11} = \int_{-h}^h C_{11}^{(k)} z^2 dz, J_{66} = \int_{-h}^h C_{66}^{(k)} z^2 dz, J_{12} = \int_{-h}^h C_{12}^{(k)} z^2 dz, \tag{B-3}$$

$$J_{22} = \int_{-h}^h C_{22}^{(k)} z^2 dz, J_{16} = \int_{-h}^h C_{16}^{(k)} z^2 dz, J_{26} = \int_{-h}^h C_{26}^{(k)} z^2 dz,$$

$$L_{11x} = \int_{-h}^h C_{11}^{(k)} \phi_x^{(k)} dz, L_{66x} = \int_{-h}^h C_{66}^{(k)} \phi_x^{(k)} dz, L_{12x} = \int_{-h}^h C_{12}^{(k)} \phi_x^{(k)} dz,$$

$$\begin{aligned}
L_{22x} &= \int_{-h}^h C_{22}^{(k)} \phi_x^{(k)} dz, L_{26x} = \int_{-h}^h C_{26}^{(k)} \phi_x^{(k)} dz, L_{16x} = \int_{-h}^h C_{16}^{(k)} \phi_x^{(k)} dz, \\
L_{22y} &= \int_{-h}^h C_{22}^{(k)} \phi_y^{(k)} dz, L_{66y} = \int_{-h}^h C_{66}^{(k)} \phi_y^{(k)} dz, L_{26y} = \int_{-h}^h C_{26}^{(k)} \phi_y^{(k)} dz, \\
L_{16y} &= \int_{-h}^h C_{16}^{(k)} \phi_y^{(k)} dz, L_{12y} = \int_{-h}^h C_{12}^{(k)} \phi_y^{(k)} dz,
\end{aligned} \tag{B-4}$$

$$\begin{aligned}
H_{66xy} &= \int_{-h}^h C_{66}^{(k)} \phi_y^{(k)} \phi_x^{(k)} dz, H_{66yy} = \int_{-h}^h C_{66}^{(k)} \phi_y^{(k)2} dz, H_{66xx} = \int_{-h}^h C_{66}^{(k)} \phi_x^{(k)2} dz, \\
H_{26xy} &= \int_{-h}^h C_{26}^{(k)} \phi_x^{(k)} \phi_y^{(k)} dz, H_{11xx} = \int_{-h}^h C_{11}^{(k)} \phi_x^{(k)2} dz, H_{22yy} = \int_{-h}^h C_{22}^{(k)} \phi_y^{(k)2} dz, \\
H_{12yx} &= \int_{-h}^h C_{12}^{(k)} \phi_y^{(k)} \phi_x^{(k)} dz, H_{16xx} = \int_{-h}^h C_{16}^{(k)} \phi_x^{(k)2} dz, H_{26yy} = \int_{-h}^h C_{26}^{(k)} \phi_y^{(k)2} dz, \\
H_{16yx} &= \int_{-h}^h C_{16}^{(k)} \phi_y^{(k)} \phi_x^{(k)} dz,
\end{aligned} \tag{B-5}$$

$$\begin{aligned}
K_{11x} &= \int_{-h}^h C_{11}^{(k)} \phi_x^{(k)} z dz, K_{66x} = \int_{-h}^h C_{66}^{(k)} \phi_x^{(k)} z dz, K_{16y} = \int_{-h}^h C_{16}^{(k)} \phi_y^{(k)} z dz, \\
K_{66y} &= \int_{-h}^h C_{66}^{(k)} \phi_y^{(k)} z dz, K_{12x} = \int_{-h}^h C_{12}^{(k)} \phi_x^{(k)} z dz, K_{22y} = \int_{-h}^h C_{22}^{(k)} \phi_y^{(k)} z dz, \\
K_{22x} &= \int_{-h}^h C_{22}^{(k)} \phi_x^{(k)} z dz, K_{12y} = \int_{-h}^h C_{12}^{(k)} \phi_y^{(k)} z dz, K_{26x} = \int_{-h}^h C_{26}^{(k)} \phi_x^{(k)} z dz,
\end{aligned} \tag{B-6}$$

$$\begin{aligned}
K_{16x} &= \int_{-h}^h C_{16}^{(k)} \phi_x^{(k)} z dz, K_{26y} = \int_{-h}^h C_{26}^{(k)} \phi_y^{(k)} z dz, \\
E_{22y} &= \int_{-h}^h Q_{22}^{(k)} \frac{\partial \phi_y^{(k)}}{\partial z} dz, E_{12y} = \int_{-h}^h Q_{12}^{(k)} \frac{\partial \phi_y^{(k)}}{\partial z} dz, \\
E_{12x} &= \int_{-h}^h Q_{12}^{(k)} \frac{\partial \phi_x^{(k)}}{\partial z} dz, E_{11x} = \int_{-h}^h Q_{11}^{(k)} \frac{\partial \phi_x^{(k)}}{\partial z} dz,
\end{aligned} \tag{B-7}$$

$$F_{12} = \int_{-h}^h Q_{12}^{(k)} dz, F_{11} = \int_{-h}^h Q_{11}^{(k)} dz, F_{22} = \int_{-h}^h Q_{22}^{(k)} dz, \tag{B-8}$$

$$P_{12yx} = \int_{-h}^h Q_{12}^{(k)} \frac{\partial \phi_y^{(k)}}{\partial z} \frac{\partial \phi_x^{(k)}}{\partial z} dz, P_{11xx} = \int_{-h}^h Q_{11}^{(k)} \left( \frac{\partial \phi_x^{(k)}}{\partial z} \right)^2 dz, P_{22yy} = \int_{-h}^h Q_{22}^{(k)} \left( \frac{\partial \phi_y^{(k)}}{\partial z} \right)^2 dz. \tag{B-9}$$

## REFERENCES

1. F. Auricchio, G. Balduzzi, M. J. Khoshgoftar, G. Rahimi, and E. Sacco, "Enhanced modeling approach for multilayer anisotropic plates based on dimension reduction method and Hellinger–Reissner principle," *Composite Structures*, **118**, 622-633 (2014).
2. M. Fares and M. K. Elmaghany, "A refined zig-zag nonlinear first-order shear deformation theory of composite laminated plates," *Composite Structures*, **82**, 71-83 (2008).
3. A. Gupta and A. Ghosh, "Bending analysis of laminated and sandwich composite reissner-mindlin plates using nurbs-based isogeometric approach," *Procedia Engineering*, **173**, 1334-1341 (2017).

4. G. Pavan and K. N. Rao, "Bending analysis of laminated composite plates using isogeometric collocation method," *Composite Structures*, **176**, 715-728 (2017).
5. R. A. Chaudhuri, "A nonlinear zig-zag theory for finite element analysis of highly shear-deformable laminated anisotropic shells," *Composite Structures*, **85**, 350-359 (2008).
6. M. J. Khoshgoftar, M. Mirzaali, and G. Rahimi, "Thermoelastic analysis of non-uniform pressurized functionally graded cylinder with variable thickness using first order shear deformation theory (FSDT) and perturbation method," *Chinese Journal of Mechanical Engineering*, **28**, 1149-1156 (2015).
7. M. J. Khoshgoftar, G. Rahimi, and M. Arefi, "Exact solution of functionally graded thick cylinder with finite length under longitudinally non-uniform pressure," *Mechanics Research Communications*, **51**, 61-66 (2013).
8. I. Kreja and R. Schmidt, "Large rotations in first-order shear deformation FE analysis of laminated shells," *International Journal of Nonlinear Mechanics*, **41**, 101-123 (2006).
9. M. Ganapathi, B. Patel, and D. Makhecha, "Nonlinear dynamic analysis of thick composite/sandwich laminates using an accurate higher-order theory," *Composites Part B: Engineering*, **35**, 345-355 (2004).
10. S. Kapuria and G. Achary, "Nonlinear zig-zag theory for electrothermomechanical buckling of piezoelectric composite and sandwich plates," *Acta Mechanica*, **184**, 61-76 (2006).
11. S. Kapuria and G. Achary, "Nonlinear coupled zig-zag theory for buckling of hybrid piezoelectric plates," *Composite Structures*, **74**, 253-264 (2006).
12. M. Amabili, "A new nonlinear higher-order shear deformation theory with thickness variation for large-amplitude vibrations of laminated doubly curved shells," *Journal of Sound and Vibration*, **332**, 4620-4640 (2013).
13. M. Amabili, "A nonlinear higher-order thickness stretching and shear deformation theory for large-amplitude vibrations of laminated doubly curved shells," *International Journal of Nonlinear Mechanics*, **58**, 57-75 (2014).
14. M. Amabili, "Non-linearities in rotation and thickness deformation in a new third-order thickness deformation theory for static and dynamic analysis of isotropic and laminated doubly curved shells," *International Journal of Nonlinear Mechanics*, **69**, 109-128 (2015).
15. S. Savithri and T. Varadan, "Large deflection analysis of laminated composite plates," *International Journal of Nonlinear Mechanics*, **28**, 1-12 (1993).
16. R. C. Averill, "Static and dynamic response of moderately thick laminated beams with damage," *Composites Engineering*, **4**, 381-395 (1994).
17. R. Averill and Y. C. Yip, "Development of simple, robust finite elements based on refined theories for thick laminated beams," *Computers & Structures*, **59**, 529-546 (1996).
18. M. Di Sciuva, "Multilayered anisotropic plate models with continuous interlaminar stresses," *Composite Structures*, **22**, 149-167 (1992).
19. M. Di Sciuva, M. Gherlone, and L. Librescu, "Implications of damaged interfaces and of other non-classical effects on the load carrying capacity of multilayered composite shallow shells," *International Journal of Nonlinear Mechanics*, **37**, 851-867 (2002).
20. A. Tessler, M. Di Sciuva, and M. Gherlone, "Refinement of Timoshenko beam theory for composite and sandwich beams using zig-zag kinematics," NASA-TP-2007-215086, National Aeronautics and Space Administration, Washington, D.C., (2007).
21. A. Tessler, M. Di Sciuva, and M. Gherlone, "Refined zig-zag theory for laminated composite and sandwich plates," NASA/TP-2009-215561, National Aeronautics and Space Administration, Washington, D.C., (2009).
22. A. Ascione and M. Gherlone, "Nonlinear static response analysis of sandwich beams using the refined zig-zag theory," *Journal of Sandwich Structures & Materials*, **22**, No. 7, 2250-2286 (2020).
23. M. Shaban and H. Mazaheri, "Size-dependent electro-static analysis of smart micro-sandwich panels with functionally graded core," *Acta Mechanica*, **232**, No. 1, 111-133 (2021).
24. M. Arefi, E. Mohammad-Rezaei Bidgoli, and T. Rabczuk, "Effect of various characteristics of graphene nanoplatelets on thermal buckling behavior of FGRC micro plate based on MCST," *European Journal of Mechanics-A/Solids*, **77**, 103802 (2019).
25. M. Arefi and M. Amabili, "A comprehensive electro-magneto-elastic buckling and bending analyses of three-layered doubly curved nanoshell, based on nonlocal three-dimensional theory," *Composite Structures*, **257**, 113100 (2021).
26. M. Arefi, E. Mohammad-Rezaei Bidgoli, and T. Rabczuk, "Thermo-mechanical buckling behavior of FG GNP reinforced micro plate based on MSGT," *Thin-Walled Structures*, **142**, 444-459 (2019).

27. E. Mohammad-Rezaei Bidgoli, and M. Arefi, "Free vibration analysis of micro plate reinforced with functionally graded graphene nanoplatelets based on modified strain-gradient formulation," *Journal of Sandwich Structures & Materials*, **23**, No. 2, 436-472 (2021).
28. M. M. Alipour, and M. Shaban, "Natural frequency and bending analysis of heterogeneous polar orthotropic-faced sandwich panels in the existence of in-plane pre-stress," *Archives of Civil and Mechanical Engineering*, **20**, No. 4, 1-24 (2020).
29. M. Shaban and H. Mazaheri, "Closed-form elasticity solution for smart curved sandwich panels with soft core," *Applied Mathematical Modelling*, **76**, 50-70 (2019).
30. M. Arefi, and F. Najafitabar, "Buckling and free vibration analyses of a sandwich beam made of a soft core with FG-GNPs reinforced composite face-sheets using Ritz method," *Thin-Walled Structures*, **158**, 107200 (2021).
31. M. Shaban and A. Alibeigloo, "Global bending analysis of corrugated sandwich panels with integrated piezoelectric layers," *Journal of Sandwich Structures & Materials*, **22**, No. 4, 1055-1073 (2020).
32. M. Arefi, "Electro-mechanical vibration characteristics of piezoelectric nano shells," *Thin-Walled Structures*, **155**, 106912 (2020).
33. M. Arefi, S. Kiani Moghaddam, E. Mohammad-Rezaei Bidgoli, M. Kiani, and O. Civalek, "Analysis of graphene nanoplatelet reinforced cylindrical shell subjected to thermo-mechanical loads," *Composite Structures*, **255**, 112924 (2021).
34. N. Pagano, "Exact solutions for composite laminates in cylindrical bending," *Journal of Composite Materials*, **3**, 398-411 (1969).